Automatic oil spill detection on quad polarimetric UAVSAR imagery

Maryam Rahnemoonfar, Shanti Dhakal

School of Engineering and Computing Sciences, Texas A&M University-Corpus Christi

ABSTRACT

Oil spill on the water bodies has adverse effects on coastal and marine ecology. Oil spill contingency planning is of utmost importance in order to plan for mitigation and remediation of the oceanic oil spill. Remote sensing technologies are used for monitoring the oil spills on the ocean and coastal region. Airborne and satellite sensors such as optical, infrared, ultraviolet, radar and microwave sensors are available for remote surveillance of the ocean. Synthetic Aperture Radar (SAR) is used most extensively for oil-spill monitoring because of its capability to operate during day/night and cloud-cover condition. This study detects the possible oil spill regions on fully polarimetric Uninhabited Aerial Vehicle - Synthetic Aperture Radar (UAVSAR) images. The UAVSAR image is decomposed using Cloude-Pottier polarimetric decomposition technique to obtain entropy and alpha parameters. In addition, other polarimetric features such as co-polar correlation and degree of polarization are obtained for the UAVSAR images. These features are used to with fuzzy logic based classification to detect oil spill on the SAR images. The experimental results show the effectiveness of the proposed method.

Keywords- oil spill, SAR, Polarimetry, Fuzzy logic

1. INTRODUCTION

Oil spills on the ocean due to accidental or deliberate actions pose a great threat to aquatic and coastal life and environment. The impact of oil spill depends upon the type and thickness of the oil [1]. Remote sensing provides great tools for monitoring oil spills on the vast oceanic areas. Several airborne and space-borne satellite images have been used to obtain images of the ocean and coastal marsh and to detect oil spill. Sensors such as infrared, ultraviolet, laser fluorosensor, radar sensors provide information about the location of the spill, area covered by the spill, type and thickness of oil, which is very useful for oil spill monitoring [2]. Every year several thousand tons of oil is spilled on the ocean water by accident, natural seepage or by illegal activities [3]. During the Deep Water Horizon (DWH) oil spill accident, from April 20, 2010 until July 15, 2010, an estimated upper limit of 1.3×10^9 L of oil and gas-oil equivalent was released to the Gulf -of-Mexico water stream [3]. When the oil is spilled on the seawater, the oil slick can emulsify, sink to the bottom, get dispersed due to the wind and/or evaporate. The oil spill in water affects marine ecosystem, declining the population of phytoplankton and other aquatic life .

Synthetic Aperture Radar (SAR) images are commonly used for oil detection. Radar sensors are very popular sensors because of their ability to operate during day, night, and adverse weather conditions.

Visual sensors cannot operate during dark, foggy and cloudy conditions as they obstruct the visibility. Also, during bright daylight, the sun glint interferes with the image clarity. Using infrared sensors, we can estimate the relative thickness of oil slicks. However, thin sheens of oil are not detectable in infrared images. Seaweeds and shorelines provide false positive result [1], [3], [4]. Oil has stronger reflectivity than water in ultraviolet region. The ultraviolet sensors can detect

Polarization: Measurement, Analysis, and Remote Sensing XII, edited by David B. Chenault, Dennis H. Goldstein,
Proc. of SPIE Vol. 9853, 985310 · © 2016 SPIE · CCC code: 0277-786X/16/$18 · doi: 10.1117/12.2223966

very thin (less than 0.1 micron) sheens of oil. However, the ultraviolet sensor cannot detect sheens greater than 10 micron in thickness.

Several efforts have been made to automate the oil detection process. The oil spill detection processes widely utilize the SAR image with single polarization. The authors in [5], [6] use fuzzy logic techniques that imitates the expert's decision making skills to automatically detect oil spills on the SAR images. They use the features such as total number of dark objects identified on the image, the area of the candidate dark object, eccentricity of the object's shape and proximity to the land as input parameter for fuzzy logic system. Oil spill detection algorithm in [7] is based upon two-phase classification. A support vector machine (SVM) is also used for classifying the SAR image into regions of oil spill and look-alikes from a set of geometrical and gray-level features extracted from the image [8]. Artificial neural networks are used to classify the dark objects in SAR image as oil spill in [9], [10], [11].

Single polarimetric SAR has an advantage of large swath coverage. However, oil spill detection in SAR with single polarization requires large number of SAR images and in-situ known oil-spill databases. Fully polarimetric SAR provides additional information that can be obtained from scattering matrices allowing discrimination of oil spill and the ocean background. Polarimetric decomposition parameters such as entropy (H), anisotropy (A), Mean scattering angle (α) can provide us some insight into oil-spill . Other parameters, such as co-polar correlation coefficient (ρ), standard deviation of co-polar phase difference (CPD), conformity index, coherence measure can also aid to oil spill detection [12], [13], [14], [15], [16], [17]. The authors in [18] used fully polarimetric UAVAR images for oil spill detection. They use four basic polarimetric parameters - co-polar correlation coefficient (ρ), entropy (H), Mean scattering angle (α) and anisotropy (A).

In this paper, Cloude-Pottier target decomposition theorem is used to obtain entropy, mean alpha and anisotropy from the fully polarimetric UAVSAR images. The correlation coefficient and degree of polarization parameters are also extracted from the SAR image. These features are used with fuzzy logic based classification to detect oil spill.

2. PROPOSED METHOD

The methodology used in this study is represented in a flowchart in Fig. 1. First, the UAVSAR images are acquired and decomposed to extract the polarimetric features such as entropy, mean alpha, anisotropy. The eigenvalues and eigenvector based Cloude-Pottier target decomposition theorem [19], [20] is used for decomposing the SAR images. The next step deals with the fuzzy classification of the regions on the image as oil spill and oil-free regions. The pixels representing oil and pixels representing water is grouped into separate clusters enabling us to discriminate oil and water.

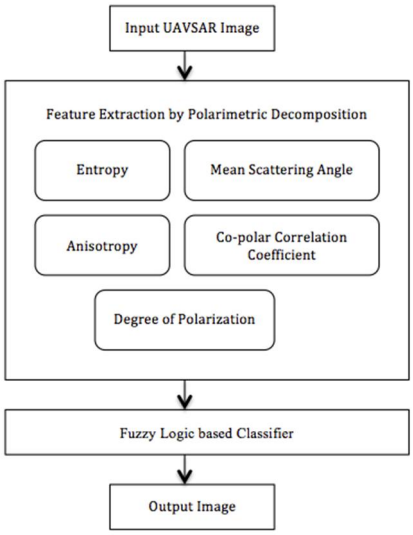

Figure 1. Flowchart of the oil-spill detection process

2.1 Feature Extraction by Polarimetric Decomposition

A polarimetric SAR can receive and transmit in two polarizations, horizontal (H) and vertical (V). A fully polarimetric SAR can transmit H polarization and receiver both H and V polarization. Similarly, it can transmit V polarization and receive both H and V polarization. The polarimetric features are extracted using Cloude Pottier target decomposition theorem [19]. These extracted features are used as input for the fuzzy classifier system.

Cloude-Pottier decomposition is the eigenvector-eigenvalue based target decomposition. It is based on the eigen decomposition of coherency matrix. The primary parameters of the eigen decomposition are the eigenvalues and the eigenvectors. The three secondary parameters, entropy, anisotropy and mean alpha, can be defined from the eigen decomposition which can be used for radar backscatter analysis of targets. Entropy (H) measures the degree of randomness of the scattering matrix. Anisotropy (A) provides the complementary information with respect to entropy. The mean scattering angle is the mean angle of the backscatter.

Entropy is the measure of randomness in the distributed scatterer and is defined from the logarithmic sum of the eigenvalues. The mean scattering angle indicates the types of scattering mechanisms present in the target. There are three types of scattering – surface, volume and double bounce. The surface scattering is seen in ocean surface and bare land surface. The volume scattering corresponds to the scattering of a dense forest canopy. The double bounce scattering corresponds to the scattering due to man-made objects such as buildings, and ships. In the ocean, surface scattering is dominant. Anisotropy measures the relative values of the second and third eigenvalues. Anisotropy can be considered as an indication of small-scale surface roughness [21].

The correlation coefficient is complex and is computed as the average of the product between the complex amplitude of the HH channel and the conjugate of the complex amplitude of the VV channel. It is normalized by the square root of the product of the power in the HH and VV channel [9].

The radar reflected from the surface of ocean follows the Bragg's scattering mechanism. Bragg's scattering takes place when short capillary waves and gravity waves reflect the radar energy. The presence of oil-slick on the ocean surface causes the dampening of the capillary waves. In such a condition, a non-Bragg scattering mechanism takes place [13]. The departure from Bragg scattering can be measured by degree of polarization (DoP), which can be used in oil-slick identification[21] . DoP deals with the amount of intensity associated to the polarized part of an electromagnetic field with respect to the total intensity [13].

2.2 Fuzzy Logic classification

Fuzzy logic theory addresses the uncertainty of any statement and handles partial-truth values. Fuzzy set theory is based upon the degree of membership. Unlike traditional set theory, where an object can take membership of one or the other set, the fuzzy set theory assigns a partial membership to the objects [22]. Each object in a fuzzy set is assigned a membership value, which is a real number between 0 and 1.

The components of the fuzzy logic system are discussed briefly below [22].

1) Knowledge base - The knowledgebase is the heart of fuzzy logic system. The knowledgebase comprises of rule base and database. The rule base consists of if-then-else rules that define the fuzzy inputs and the fuzzy outputs based on the conditions and actions associated with fuzzy inputs.

2) Fuzzification - The input to the fuzzy logic is a crisp value. The Fuzzification process assigns one or more fuzzy sets to the crisp inputs, producing the fuzzy variables, which now can take membership to one or more fuzzy sets.

3) Inference - The fuzzy inputs are then processed using if-then-else rules from the Knowledgebase. The fuzzy outputs are inferred from the fuzzy inputs using the inference from the knowledgebase.

4) Defuzzification – The fuzzy outputs from the inference process is converted back to crisp values by averaging and weighting the individual outputs of fuzzy rules into a single crisp output.

The polarimetric features obtained from the SAR images are used as input in the fuzzy logic classification system. The fuzzy classifier is used for discriminating oil spill region from look-alikes. The development of fuzzy classifier involves the following three steps.

1) Input parameters: The first step in developing fuzzy classifier is to select a set of input parameters for classification. The polarimetric features - entropy, anisotropy, mean-alpha, co-polar correlation coefficient and degree of polarization are selected as input for the fuzzy classifier.

2) Fuzzy sets: Three fuzzy sets - "low", "medium" and "high", are defined for all the input variables. The co-polar correlation coefficient, entropy and anisotropy are defined over the degree of membership from 0 to 1. Similarly, three fuzzy sets for alpha is developed with values ranging from 0° - 90°.

3) Rule base: The oil on water surface is characterized by high entropy low mean alpha and co-polar correlation coefficient. There are several rules like this. In this research, a combination of 12 rules were used for oil spill classification.

3. EXPERIMENTAL RESULTS

The UAVSAR data used for the study was obtained from NASA UAVSAR instrument. The UAVSAR is an aircraft with fully polarimetric L-band SAR, which operates on 80 MHz bandwidth. UAVSAR images are obtained at 22° - 65° incident angles. The UAVSAR data used for this study is a Multi-Look Complex (MLC) fully polarimetric UAVSAR images which were acquired during the Deep Water Horizon (DWH) oil rig. Several UAVSAR Data set were used in his project. Here we just focus on gulfco_32010_ 10054_101_100623 taken on 23-June-2010 at 21:08 UTC. The UAVSAR images shown in this paper are in slant range and azimuth coordinate system.

Figure 2 shows the Pauli color-coded image of the dataset used in this study. In Pauli color-coding, the polarimetric information of scattering matrix, is represented by the combination of the intensities $|S_{HH}|^2$, $|S_{VV}|^2$ and $2|S_{HV}|^2$ in a single RGB image, i.e., every of the previous intensities coded as a color channel. Hence, $|S_{HH} + S_{VV}|$ is represented by blue color, $|S_{HH} - S_{VV}|$ is represented by red color and $|S_{HV}|$ is represented by green color. The $|S_{HH} + S_{VV}|$ represents single scattering, $|S_{HH} - S_{VV}|$ represents double bounce scattering and $|S_{HV}|$ represents volume scattering. Features are extracted from input image using Cloude-Pottier polarimetric decomposition. The extracted features, entropy, anisotropy and alpha (H/A/alpha), co-polar correlation coefficient, and degree of polarization were entered to the fuzzy logic classifier to classify the region of the image as oil spill and oil-free regions. Figures 3 shows the entropy, mean-alpha, anisotropy, co-polar correlation coefficient, and degree of polarization images of the image. The co-polar correlation coefficient, degree of polarization, entropy and anisotropy values ranges from 0 (blue) to 1 (red). The mean alpha values ranges from 0° (blue) - 90°(red).

Figure 2. Pauli color-coded image $|S_{HH} - S_{VV}||S_{HV}||S_{HH} + S_{VV}|$ of the image

Ocean surface is regarded as low entropy region as compared to land and urban areas because of a single surface scattering. However, the presence of oil on water increases the entropy because of multi-scattering of radar signal [12]. The entropy of the image is shown in fig 3(a). The red color represents high entropy while blue color represents low entropy. The oil-free water surface has lower entropy as compared to surface covered by oil. The mean alpha is shown in fig 3(b). Low alpha signifies a presence of a single dominant scatterer [21]. The anisotropy of image is shown in fig 3(c). Anisotropy is a level of dominance between second and third scattering mechanism. So, anisotropy is useful to determine whether there is second or third scattering mechanism present [21].

There is a high HH-VV correlation in oil-free water surface, the co-polar correlation coefficient in oil-free water is higher than in the oil-covered region [18]. The co-polar correlation coefficient is shown in fig 3(d).

In a slick-free surface, Bragg's scattering mechanism takes place, hence, there is low level of depolarization of the radar backscatter [13], [14]. The DoP in such case, is close to 1. However, the presence of oil slick on the water is characterized by non-Bragg scattering, so, there is a large depolarization of radar backscatter. In such cases, DoP is estimated to be close to 0. DOP is presented in fig 3(e). The output of the fuzzy classifier is shown in figure 3(f). The red and yellow region on the top part of the image shows the oil spill region. The red region represents higher probability of oil spill. The red region in the bottom and middle section of the image is the land region. The blue region on the image represents water. The dark regions in Pauli color-coded image in figure 2 that are not classified as oil in figure 3f, are the look-alikes.

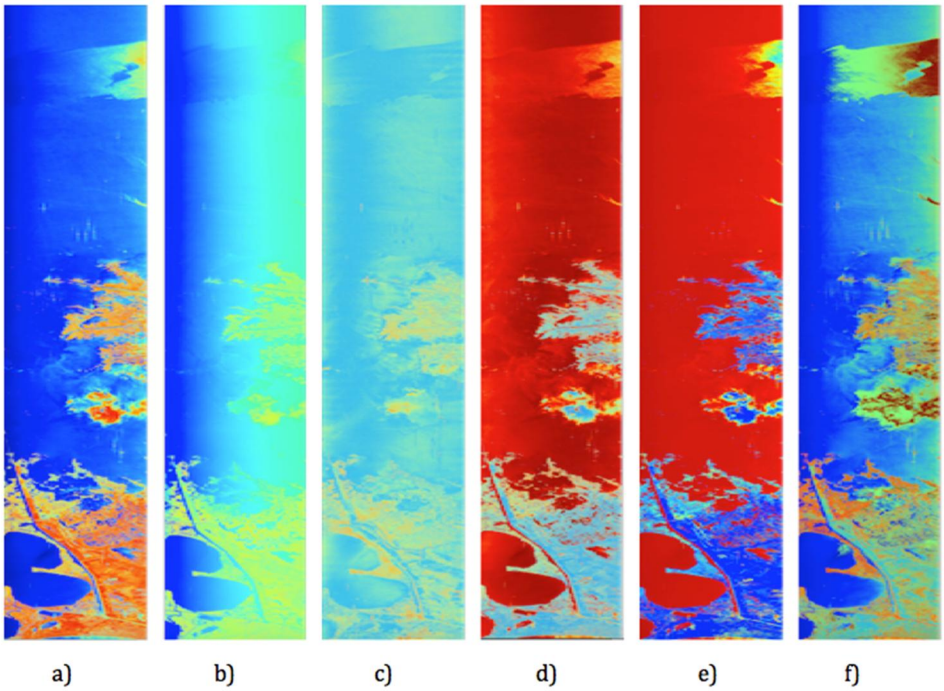

Figure 3 Polarimetric Decomposition of the image. a) entropy, b) mean alpha c) anisotropy, d) co-polar correlation coefficient, e) degree of polarization, f) output of fuzzy classifier.

4. CONCLUSION

SAR images are the most commonly used images for oil spill detection because of their capability to penetrate through cloud and operate during day and night. Since, the backscatter from the radar sensor is highly affected by the wind

condition, sea-state, and biogenic films present on the sea surface, the oil detection process is a very complicated process with large number of false-positive detection rates. The polarimetric SAR images are found to be the best choice for automatic oil-spill detection among other images. In this study, the fuzzy-logic based classification is used to discriminate the oil-spill on the UAVSAR images from look-alikes. The Cloude-Pottier target decomposition theorem is used to obtain H, A and alpha images along with co-polar correlation coefficient and degree of polarization, that are used as input parameters for fuzzy classifier. The result shows that fuzzy logic based classification is able to distinguish oil from water automatically.

5. REFERENCES

[1] A. Solberg, "Remote sensing of ocean oil-spill pollution," *Proc. IEEE*, vol. 100, no. 10, 2012.

[2] M. Jha, J. Levy, and Y. Gao, "Advances in remote sensing for oil spill disaster management: state-of-the-art sensors technology for oil spill surveillance," *Sensors*, pp. 236–255, 2008.

[3] I. Leifer, W. J. Lehr, D. Simecek-Beatty, E. Bradley, R. Clark, P. Dennison, Y. Hu, S. Matheson, C. E. Jones, B. Holt, M. Reif, D. a. Roberts, J. Svejkovsky, G. Swayze, and J. Wozencraft, "State of the art satellite and airborne marine oil spill remote sensing: Application to the BP Deepwater Horizon oil spill," *Remote Sens. Environ.*, vol. 124, pp. 185–209, Sep. 2012.

[4] M. Fingas and C. Brown, "Review of oil spill remote sensing.," *Mar. Pollut. Bull.*, vol. 83, no. 1, pp. 9–23, Jun. 2014.

[5] I. Keramitsoglou, C. Cartalis, and C. T. Kiranoudis, "Automatic identification of oil spills on satellite images," *Environ. Model. Softw.*, vol. 21, no. 5, pp. 640–652, May 2006.

[6] P. Liu and C. Zhao, "Oil Spill Identification in Marine SAR Images Based on Texture Feature and Fuzzy Logic System," *2009 Sixth Int. Conf. Fuzzy Syst. Knowl. Discov.*, pp. 433–437, 2009.

[7] S. Singha, M. Vespe, and O. Trieschmann, "Automatic Synthetic Aperture Radar based oil spill detection and performance estimation via a semi-automatic operational service benchmark.," *Mar. Pollut. Bull.*, vol. 73, no. 1, pp. 199–209, Aug. 2013.

[8] M. Cococcioni, L. Corucci, A. Masini, and F. Nardelli, "SVME: an ensemble of support vector machines for detecting oil spills from full resolution MODIS images," *Ocean Dyn.*, vol. 62, no. 3, pp. 449–467, Jan. 2012.

[9] O. Garcia-Pineda and I. MacDonald, "Oil spill mapping and measurement in the Gulf of Mexico with Textural Classifier Neural Network Algorithm (TCNNA)," IEEE Journal of Selected Topics in Applied Earth Observations and Remote Sensing , vol. 6, no. 6, pp. 2517–2525, 2013.

[10] F. Del Frate and A. Petrocchi, "Neural networks for oil spill detection using ERS-SAR data," *... Remote Sens. ...*, vol. 38, no. 5, pp. 2282–2287, 2000.

[11] F. Del Frate and L. Salvatori, "Oil spill detection by means of neural networks algorithms: a sensitivity analysis," *Geosci. Remote Sens. ...*, vol. 00, no. C, pp. 1370–1373, 2004.

[12] W. Wenguang, L. Fei, W. Peng, and W. Jun, "Oil spill detection from polarimetric SAR image," *IEEE 10th Int. ...*, pp. 832–835, 2010.

[13] F. Nunziata, A. Gambardella, and M. Migliaccio, "On the degree of polarization for SAR sea oil slick observation," *ISPRS J. Photogramm. Remote Sens.*, vol. 78, pp. 41–49, Apr. 2013.

[14] R. Shirvany, M. Chabert, and T. Jean-Yves, "Ship and oil-spill detection using the degree of polarization in linear and hybrid/compact dual-pol SAR," IEEE Journal of Selected Topics in Applied Earth Observations and Remote Sensing , vol. 5, no. 3, pp. 885–892, 2012.

[15] A.-B. Salberg, O. Rudjord, and A. H. S. Solberg, "Oil Spill Detection in Hybrid-Polarimetric SAR Images," *IEEE Trans. Geosci. Remote Sens.*, vol. 52, no. 10, pp. 6521–6533, Oct. 2014.

[16] W. Wenguang, L. Fei, W. Peng, and W. Jun, "Oil spill detection from polarimetric SAR image," *IEEE 10th Int. Conf. SIGNAL Process. Proc.*, pp. 832–835, Oct. 2010.

[17] A. H. S. Solberg, "Remote Sensing of Ocean Oil-Spill Pollution," *Proc. IEEE*, vol. 100, no. 10, pp. 2931–2945, Oct. 2012.

[18] P. Liu, X. Li, J. J. Qu, W. Wang, C. Zhao, and W. Pichel, "Oil spill detection with fully polarimetric UAVSAR data.," *Mar. Pollut. Bull.*, vol. 62, no. 12, pp. 2611–8, Dec. 2011.

[19] S. R. Cloude and E. Pottier, "A Review of Target Decomposition Theorems in Radar Polarimetry," vol. 34, no. 2, pp. 498–518, 1996.

[20] C. Lopez-Martinez, "Statistical assessment of eigenvector-based target decomposition theorems in radar polarimetry," *Geosci. Remote ...*, vol. 00, no. 4, pp. 192–195, 2005.

[21] B. Minchew, C. E. Jones, and B. Holt, "Polarimetric Analysis of Backscatter From the Deepwater Horizon Oil Spill Using L-Band Synthetic Aperture Radar," *IEEE Trans. Geosci. Remote Sens.*, vol. 50, no. 10, pp. 3812–3830, Oct. 2012.

[22] J. Yen, "Fuzzy logic-a modern perspective," *Knowl. Data Eng. IEEE Trans.*, vol. 11, no. 1, pp. 153–165, 1999.